RSC Advances

PAPER

View Article Online
View Journal | View Issue

Cite this: *RSC Adv.*, 2017, **7**, 1818

Collector and binder-free high quality graphene film as a high performance anode for lithium-ion batteries†

LianSheng Jiao,[ab] Zhonghui Sun,[a] HongYan Li,[a] Fenghua Li,[a] Tongshun Wu*[a] and Li Niu*[a]

Received 1st November 2016
Accepted 9th December 2016

DOI: 10.1039/c6ra26111f

www.rsc.org/advances

Collector and binder-free high quality graphene film has been successfully synthesized by a simple filtration process. Electrochemical results indicate that the graphene film exhibits good rate and cycle behavior compared with the commercial mesocarbon microbeads (MCMB)/copper system. More importantly, after excluding the dead-weight copper collector, the gravimetric energy density could be enhanced to some extent. This may provide an alternative in the demand for higher energy density lithium-ion batteries.

In the present era of lithium ion batteries (LIBs), there is demand for higher energy densities to power mobile electronic devices with higher power consumption and to improve the driving endurance of EVs.[1] The energy density is dependent on the specific capacities and potential difference of the anode and the cathode, so seeking active materials displaying higher specific capacities, with higher potential for the cathode and lower potential for the anode have been the main focus in this research field. In the case of the anode, tin-based and silicon-based anodes possessing relatively high capacities compared to graphite have attracted researchers' attention.[2] However, a very large irreversible capacity in the first cycle and fast capacity fading in the following cycles due to the so-called pulverization effects and high cost greatly limit their practical use.[3] In other words, an increase in the energy density cannot be fulfilled by utilizing these high capacity materials at least for the time being and other routes have to be found to improve the energy density.

As is well known, commercial mesocarbon microbead (MCMB) anode materials mixed with binders and conductive additives are usually coated on a copper (Cu) foil through a doctor blade method. In general, the weight of binders, conductive additives and current collectors, should be less 10 wt% of the total electrode because they commonly contribute no capacity. The polarization of the electrodes can be increased in the presence of binders because they not only decrease the electrical conductivity, but prevent the access of ions to the active materials as well.[4] The Cu current collector provides the structural support for the electrode and an electrical conductive pathway to active materials. It is estimated that the areal density of Cu foil (10 μm) is about 10 mg cm^{-2}. This copper component is considerably heavy, accounting for about 10% of the total weight of the cell[5] and will reduce the gravimetric energy density of the whole battery. For example, a 10 μm copper collector makes up about 45% of the weight of the anode side if the copper foil was double-coated with an areal density of 6.0 mg cm^{-2}. Thus, gravimetric energy density will be increased by about 45% on the anode side if graphene film electrode without copper collector was used. So, higher energy density can be achieved if the dead-weight Cu collector is excluded from the electrode. However, powdered MCMB material cannot form free-standing electrodes without the support of the Cu collector so other carbon-based materials have to be found.

Graphene, an extraordinary carbon nanostructure obtained by exfoliating graphite, has opened up new prospects as a candidate anode material for LIBs[6] since its first isolation in 2004. Graphene can also directly act as a flexible anode in the form of graphene paper or a membrane, which is simply obtained by vacuum filtration of a reduced graphene oxide (rGO) dispersion or chemical vapor deposition (CVD) method[7] and high capacities compared to graphite have been reported. Nevertheless, the most capacity has been achieved at potentials of 1–3.0 V, making them impossible to use as an anode in commercial use.[8] More importantly, large hysteresis, which is mainly caused by Li storage on defects such as edges and/or oxygen- and hydrogen-containing surface groups,[9] has been observed in the cycling performance of these electrodes. This voltage hysteresis will result in poor energy efficiency of the cells.[10] Thus, preparing high quality graphene with improved performance favorable for practical use is crucial.

[a]*State Key Laboratory of Electroanalytical Chemistry, CAS Center for Excellence in Nanoscience, c/o Engineering Laboratory for Modern Analytical Techniques, Changchun Institute of Applied Chemistry, Chinese Academy of Sciences, University of Chinese Academy of Sciences, Changchun 130022, Beijing, 100049, P. R. China. E-mail: lniu@ciac.ac.cn; Fax: +86 431 85262800; Tel: +86 431 85262425*

[b]*Department of Chemistry, Hebei Normal University for Nationalities, Chengde 067000, P. R. China*

† Electronic supplementary information (ESI) available. See DOI: 10.1039/c6ra26111f

In this paper, high quality graphene sheets were first synthesized by a microwave-assisted pre-exfoliation of graphite and subsequent liquid-phase exfoliation (the details are described in the ESI†). Then, collector and binder-free graphene film without a copper current collector was successfully obtained by simple vacuum filtration of the mixture of the as-prepared graphene sheets, nanocarbon fiber and carbon black in ethanol with a mass ratio of 80 : 10 : 10. Compared with the commercial mesocarbon microbead (MCMB)/copper system in lithium-ion batteries, such film acting as both an anode-active material and current collector exhibited enhanced electrochemical performance, and thus will lead to a higher energy density.

The schematic synthesis process and the structural characterization such as SEM, TEM, XRD, Raman and XPS of graphene sheets (GS) have been described in detail in our previous work.[11] The thickness of the graphene used in this work was estimated to be less than 5 layers according to the 2D band (~2700 cm^{-1}) which is characteristic of few layer graphene (Fig. S1 in the ESI†).[12] Collector and binder-free high quality graphene film (preparation process is schematically illustrated in Fig. 1) was also characterized by XRD, XPS and Raman spectroscopy, as shown in Fig. 2. The film exhibits almost the same features as those of GS, indicating that the GS maintained their basic characteristics during the subsequent mixing and filtration process. However, a blue shift of the 2D band occurs indicating that the GS folded with arbitrary orientation to some extent during filtration.[13] The areal density and the thickness of the electrode are about 3.5 mg cm^{-2} and 60 μm, respectively. The electrical conductivity of the film was measured using the four-point probe technique and was estimated to be as high as ~1100 S m^{-1} which is consistent with Cheng's report.[14]

Fig. 3a shows the first three cyclic voltammetry (CV) curves of the as-obtained graphene film in the voltage of 0.01–3.0 V at a scan rate of 1 mV s^{-1}, which is consistent with that of graphene[11] and MCMB (Fig. S2 in the ESI†). In the first scan, two broad reduction peaks located at about 1.33 V and 0.60 V were ascribed to the decomposition of ethylene carbonate solvent[15] and the formation of solid electrolyte interphase (SEI) films,[16] respectively. The formation of SEI mostly accounts for the irreversible capacity of carbonaceous materials during the first cycle. Another reduction peak below 0.2 V corresponded to the insertion of Li^+ into the graphene film electrode, while the oxidation peak at 0.35 V could be ascribed to the de-insertion of Li^+ from the electrode. Fig. 3b displays the first charge–discharge curve of the as-obtained graphene film electrode conducted between 0.005 and 1.2 V *vs.* Li^+/Li at 0.1C. The initial charge capacity is 643 mA h g^{-1} with a reversible discharge capacity of 352 mA h g^{-1}. The coulombic efficiency of the first cycle is low compared with that of the commercial MCMB/copper system (Fig. S3 in the ESI†), which may be due to more SEI films formed in graphene film having a large specific surface area and partial re-stacking of graphene layers.[17] Nevertheless, the first-cycle irreversible capacity is much lower than those in the literature,[7] which may be a result of the very few defects in the as-obtained graphene sheets.[9] Moreover, there exists a distinct potential plateau in the charge–discharge curve, which is quite different from that prepared by the RGO and CVD method. The mechanism of lithium insertion can be

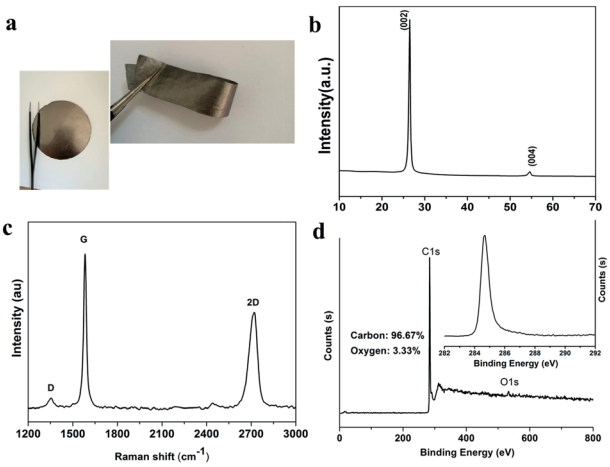

Fig. 2 (a) Optical image, (b) XRD patterns, (c) Raman spectra and (d) XPS spectra of the as-prepared graphene film.

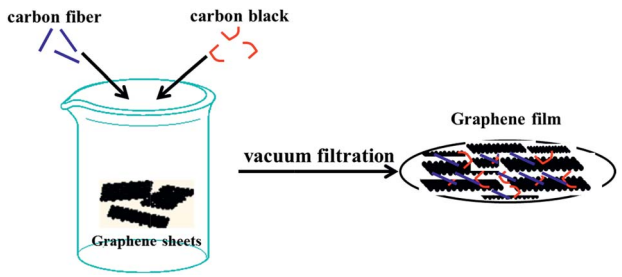

Fig. 1 Schematic illustration of the synthesis route for graphene film.

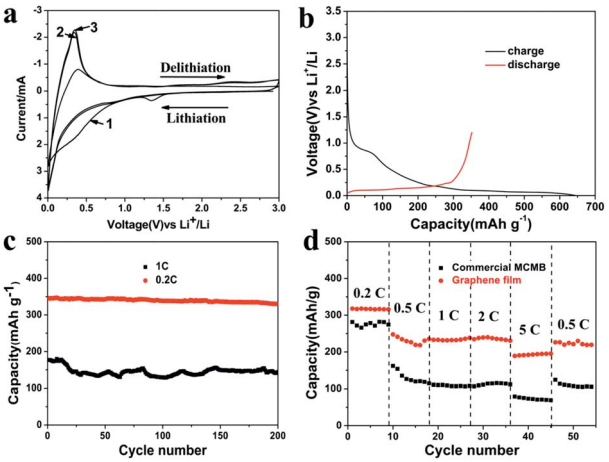

Fig. 3 (a) Cyclic voltammetry profiles of the as-obtained graphene film at a 1 mV s^{-1} scan rate (voltage range: 0.01–3.0 V) and (b) galvanostatic charge–discharge curves for the first cycle cycled between 0.01 V and 1.2 V *versus* Li^+/Li at 0.1C. (c) Cycling performance of the as-obtained graphene film at different current densities and (d) rate capability of the as-obtained graphene film and the commercial MCMB/copper system.

concluded from the staging behaviour observed in the charge–discharge profiles, namely, it reaches into the formation of LiC_6 (ref. 18) by intercalating within graphene layers progressively. No obvious voltage hysteresis in the voltage profile, indicating few edge defects and very few extrinsic oxygen- and hydrogen-containing surface groups, makes it appropriate for practical utilization.

Discharge capacities of 330 mA h g^{-1} at 0.2C and 143 mA h g^{-1} at 1C can be retained after 200 cycles (Fig. 3c), which are also much better than those of the commercial MCMB/system (Fig. S4 in the ESI†) and indicate better cycling performance with low coulombic inefficiency (Fig. S5 in the ESI†), which was associated with the excellent structural stability during the charge and discharge process. The MCMB electrode has been rolled to almost the same thickness of the graphene electrode. At 0.2C, volume changes (10%) in the MCMB electrode and some side effects between the electrolyte and inactive materials such as binders during lithiation/delithiation resulted in poor cycling stability to some extent. When the current density increased to 1C, the specific capacity experienced a dramatic fading because the electrical conductivity decreased due to the presence of binders which prevent the access of ions to the surface of the active materials. The as-obtained graphene film also demonstrates good rate capability. Reversible capacities of 316, 235, 233, 230 and 195 mA h g^{-1} can be delivered at various rates from 0.2C to 0.5C, 1 C, 2C and 5C, respectively (Fig. 3d). The good electrochemical performance of the as-prepared graphene film could be ascribed to the high electrical conductivity and a rapid charge transfer reaction for lithium ion insertion and extraction[7a] resulting from a relatively large contact area between the electrolyte and the film electrode.

In order to evaluate the potential applications of the graphene film, the issue of large first-cycle irreversible capacity related to more solid electrolyte interphase (SEI) films has been successfully addressed by a suitable prelithiation treatment by directly contacting the electrode with Li foil wetted by the electrolyte solution[19] for 2 h. The prelithiation occurred once the Li foil and graphene film were shorted and a battery shorting mechanism has been put forward in Cui's report.[20] Fig. 4a and b compare the voltage profiles of the first charge–discharge cycle of a lithium cell using a primitive graphene film electrode and a surface-treated graphene film electrode, showing the beneficial effect of the prelithiation treatment. In the first cycle, a considerably large irreversible capacity (due to the formation of more SEI films in materials with larger specific surface area) and a relatively low coulombic efficiency amounting to 60% are shown in Fig. 4a. Thereafter, the electrode delivers a stable reversible capacity of 340–350 mA h g^{-1}, associating with the electrochemical process involving lithium insertion/disinsertion into graphene layers. A remarkable reduction of the irreversible capacity and a high coulombic efficiency of 97.4% can be achieved (shown in Fig. 4b). Moreover, the pretreated graphene cell has a lower open circuit voltage (~0.2 V) than that of the regular graphene cell (~3.0 V), indicating that SEI has been formed during the *ex situ* lithiation process,[19a] which can be further confirmed by the SEM images shown in Fig. 4c and d. Solid electrolyte interphase (SEI) films

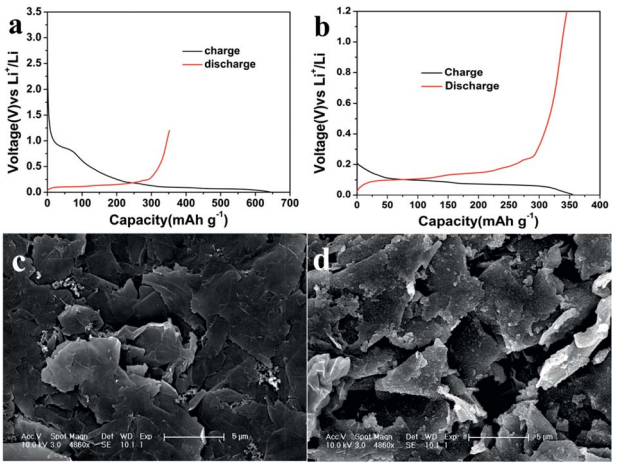

Fig. 4 Galvanostatic charge–discharge curves for the first cycle between 0.01 V and 1.2 V *versus* Li^+/Li at 0.1C of the as-obtained graphene film before (a) and after (b) surface treatment. SEM images of the film before (c) and after (d) surface treatment.

are made up of insoluble granular particles arising from the decomposition of the electrolyte solvent.[21] The cycling and rate performance of the two cells have also been compared. As can be seen in Fig. 5a and b, the cell using a surface-treated graphene film electrode displays somewhat better electrochemical performance than that of the pristine graphene film, demonstrating that this electrode can indeed operate under a high rate and can keep a stable capacity at a current of 1C after 200 cycles and can find its application in practical lithium ion batteries. The graphene electrode will indeed experience volume changes (10%) during lithiation/delithiation. Fortunately, the flexibility of graphene sheet can effectively buffer and compensate volume changes. Meanwhile, the film possesses a higher mechanic strength with a tensile modulus of 540 MPa. Thus, good connection can be maintained during the charge/discharge process.

In summary, collector and binder-free high quality graphene film has been successfully synthesized by a simple filtration process after the graphene sheets were synthesized by a solid-exfoliation of graphite and a subsequent wet chemical method. The nanocarbon fibers were selected as the scaffolds, not only to reinforce the mechanical flexibility of the film, but to separate the graphene sheets from compactly re-stacking as

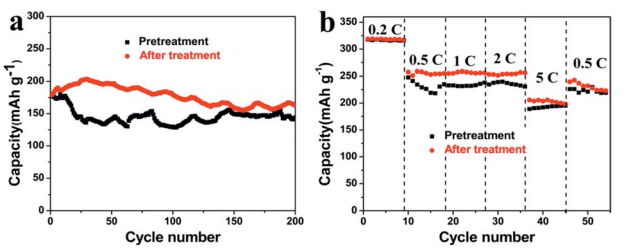

Fig. 5 Cycling performance of the galvanostatic test run at a rate of 1C (a) and at various C-rates (b) of the graphene film before and after a surface treatment.

well. When used as anode materials in lithium-ion batteries, the as-obtained graphene film not only exhibited enhanced electrochemical performance compared with commercial MCMB/copper system, but showed a satisfactory charge–discharge profile. The initial coulombic efficiency has been improved by an effective pre-lithiation strategy. More important, after excluding the dead-weight copper collector, the gravimetric energy density could be enhanced to some extent. This may provide an alternative in the demand for higher energy density of lithium-ion batteries.

Acknowledgements

This work was supported by the NSFC, China (No. 21375124, No. 21405147, No. 21225524 and No. 21475122), the Department of Science and Techniques of Jilin Province (No. 20120308, No. 201215091 and SYHZ0006) and the Chinese Academy of Sciences (YZ201354, YZ201355).

Notes and references

1 J. W. Choi and D. Aurbach, *Nature Reviews Materials*, 2016, **1**, 16013.

2 (*a*) N. Liu, K. Huo, M. T. McDowell, J. Zhao and Y. Cui, *Sci. Rep.*, 2013, **3**, 1919; (*b*) X. Wang, X. Cao, L. Bourgeois, H. Guan, S. Chen, Y. Zhong, D.-M. Tang, H. Li, T. Zhai, L. Li, Y. Bando and D. Golberg, *Adv. Funct. Mater.*, 2012, **22**, 2682; (*c*) K. Evanoff, A. Magasinski, J. Yang and G. Yushin, *Adv. Energy Mater.*, 2011, **1**, 495; (*d*) H. Ma, F. Cheng, J. Y. Chen, J. Z. Zhao, C. S. Li, Z. L. Tao and J. Liang, *Adv. Mater.*, 2007, **19**, 4067.

3 V. Etacheri, R. Marom, R. Elazari, G. Salitra and D. Aurbach, *Energy Environ. Sci.*, 2011, **4**, 3243.

4 G. Zhou, F. Li and H.-M. Cheng, *Energy Environ. Sci.*, 2014, **7**, 1307.

5 L.-F. Cui, L. Hu, J. W. Choi and Y. Cui, *ACS Nano*, 2010, **4**, 3671.

6 (*a*) W. Ahn, H. S. Song, S.-H. Park, K.-B. Kim, K.-H. Shin, S. N. Lim and S.-H. Yeon, *Electrochim. Acta*, 2014, **132**, 172; (*b*) Y. Hu, X. Li, D. Geng, M. Cai, R. Li and X. Sun, *Electrochim. Acta*, 2013, **91**, 227; (*c*) L. Wan, Z. Ren, H. Wang, G. Wang, X. Tong, S. Gao and J. Bai, *Diamond Relat. Mater.*, 2011, **20**, 756; (*d*) G. Wang, X. Shen, J. Yao and J. Park, *Carbon*, 2009, **47**, 2049; (*e*) H. Wang, H. Peng, G. Li and K. Chen, *Chem. Eng. J.*, 2015, **275**, 160; (*f*) J.-f. Zhang, X.-w. Wang, B. Zhang and Z.-h. Yang, *Electrochim. Acta*, 2015, **169**, 462; (*g*) P. Lian, X. Zhu, S. Liang, Z. Li, W. Yang and H. Wang, *Electrochim. Acta*, 2010, **55**, 3909; (*h*) S. Yin, Y. Zhang, J. Kong, C. Zou, C. M. Li, X. Lu, J. Ma, F. Y. C. Boey and X. Chen, *ACS Nano*, 2011, **5**, 3831.

7 (*a*) G. Ning, C. Xu, Y. Cao, X. Zhu, Z. Jiang, Z. Fan, W. Qian, F. Wei and J. Gao, *J. Mater. Chem. A*, 2013, **1**, 408; (*b*) C. Wang, D. Li, C. O. Too and G. G. Wallace, *Chem. Mater.*, 2009, **21**, 2604.

8 D. Choi, W. Wang and Z. Yang, in *Lithium-Ion Batteries*, CRC Press, 2011, pp. 1–50.

9 H. F. Xiang, Z. D. Li, K. Xie, J. Z. Jiang, J. J. Chen, P. C. Lian, J. S. Wu, Y. Yu and H. H. Wang, *RSC Adv.*, 2012, **2**, 6792.

10 R. Raccichini, A. Varzi, S. Passerini and B. Scrosati, *Nat. Mater.*, 2015, **14**, 271.

11 L. Jiao, T. Wu, H. Li, F. Li and L. Niu, *Chem. Commun.*, 2015, **51**, 15979.

12 (*a*) A. C. Ferrari, J. C. Meyer, V. Scardaci, C. Casiraghi, M. Lazzeri, F. Mauri, S. Piscanec, D. Jiang, K. S. Novoselov, S. Roth and A. K. Geim, *Phys. Rev. Lett.*, 2006, **97**, 187401; (*b*) K. R. Paton, E. Varrla, C. Backes, R. J. Smith, U. Khan, A. O'Neill, C. Boland, M. Lotya, O. M. Istrate, P. King, T. Higgins, S. Barwich, P. May, P. Puczkarski, I. Ahmed, M. Moebius, H. Pettersson, E. Long, J. Coelho, S. E. O'Brien, E. K. McGuire, B. M. Sanchez, G. S. Duesberg, N. McEvoy, T. J. Pennycook, C. Downing, A. Crossley, V. Nicolosi and J. N. Coleman, *Nat. Mater.*, 2014, **13**, 624.

13 Y. Hao, Y. Wang, L. Wang, Z. Ni, Z. Wang, R. Wang, C. K. Koo, Z. Shen and J. T. L. Thong, *Small*, 2010, **6**, 195.

14 N. Li, Z. Chen, W. Ren, F. Li and H.-M. Cheng, *Proc. Natl. Acad. Sci. U. S. A.*, 2012, **109**, 17360.

15 (*a*) J. B. Goodenough and Y. Kim, *Chem. Mater.*, 2010, **22**, 587; (*b*) J.-C. Panitz, U. Wietelmann, M. Wachtler, S. Ströbele and M. Wohlfahrt-Mehrens, *J. Power Sources*, 2006, **153**, 396; (*c*) X. Zhang, R. Kostecki, T. J. Richardson, J. K. Pugh and P. N. Ross, *J. Electrochem. Soc.*, 2001, **148**, A1341.

16 M. Winter, J. O. Besenhard, M. E. Spahr and P. Novák, *Adv. Mater.*, 1998, **10**, 725.

17 D. Pan, S. Wang, B. Zhao, M. Wu, H. Zhang, Y. Wang and Z. Jiao, *Chem. Mater.*, 2009, **21**, 3136.

18 (*a*) J. R. Dahn, T. Zheng, Y. Liu and J. S. Xue, *Science*, 1995, **270**, 590; (*b*) A. Ricardo, L. Pedro, P.-V. Carlos and L. T. José, in *Lithium-Ion Batteries*, CRC Press, 2011, pp. 97–146.

19 (*a*) J.-S. Bridel, S. Grugeon, S. Laruelle, J. Hassoun, P. Reale, B. Scrosati and J.-M. Tarascon, *J. Power Sources*, 2010, **195**, 2036; (*b*) J. Hassoun, F. Bonaccorso, M. Agostini, M. Angelucci, M. G. Betti, R. Cingolani, M. Gemmi, C. Mariani, S. Panero, V. Pellegrini and B. Scrosati, *Nano Lett.*, 2014, **14**, 4901.

20 N. Liu, L. Hu, M. T. McDowell, A. Jackson and Y. Cui, *ACS Nano*, 2011, **5**, 6487.

21 S. Megahed and B. Scrosati, *J. Power Sources*, 1994, **51**, 79.